OHMIC BIFURCATED STATES IN RTP

M.R. de Baar, B.H. Deng, G.M.D. Hogeweij, N.J. Lopes Cardozo, and the RTP team

FOM-Instituut voor Plasmafysica "Rijnhuizen", Association Euratom-FOM, Trilateral Euregio Cluster, P.O. Box 1207, 3430 BE Nieuwegein, the Netherlands

1. Introduction

For low n_e Ohmic tokamak plasmas τ_E is proportional to n_e (LOC) while above a threshold (typically $n_e = 5 \times 10^{19} m^{-3}$) τ_E becomes independent of n_e (SOC). In both regimes the q-profile reaches just below unity in the center of the discharge. The T_e and j-profiles are peaked and are coupled through the resistivity, which is a function of T_e.

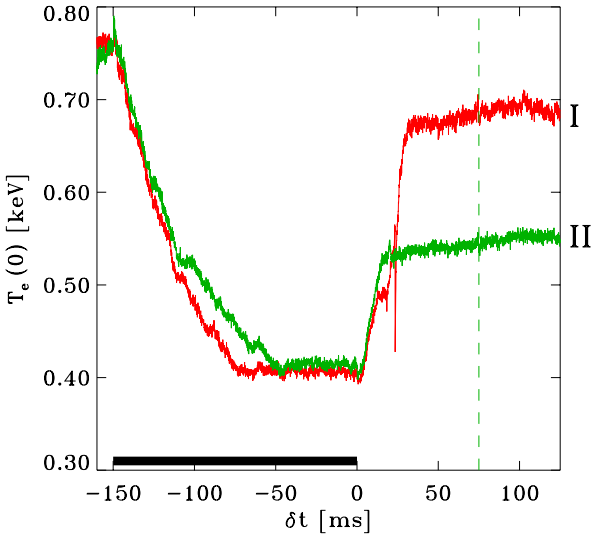

Figure 1. Evolution of $T_e(\rho = 0, t)$ for two discharges. Note, that after switch-off of the ECH system ($\delta t > 0$ ms), two distinct branches form. State I discharges show an instability (here at $\delta t = 18$ ms) after which the two states diverge.

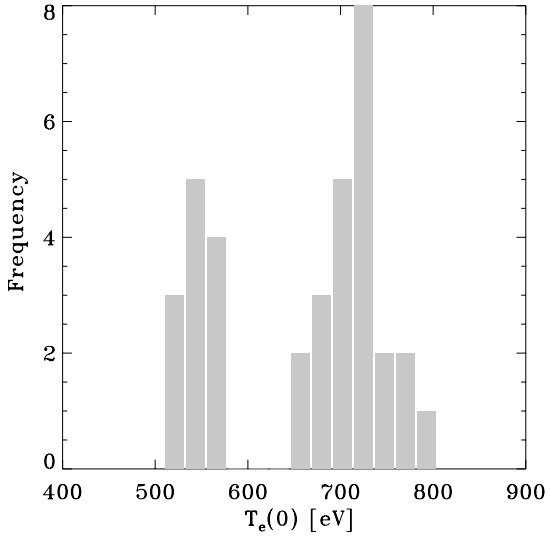

Figure 2. Database of relaxed Ohmic states. The gap around 600 eV shows the existence of the two states.

In RTP ($R_0 = 0.72$ m, $a = 0.164$ m, $B_\phi(\rho = 0) \leq 2.45$ T, $I_p \leq 140$ kA, $n_e(0)$ between 0.5×10^{19} and 1.5×10^{20}) the T_e-profile can be manipulated with a 110 GHz., 500 kW system for second harmonic X-mode operation. L-mode discharges are produced with dominant ECH. Moreover, a critical dependence of the local confinement on the EC-power deposition radius was observed [1].

The present paper reports on post off-axis ECH discharges in LOC. Depending on the history of the discharge two bifurcated states can be reached. In addition to the normal Ohmic state with a peaked T_e-profile and central q touching unity, a new state has been measured with a much broader T_e-profile, a q-profile which stays well above unity, and a very unusual n_e-profile, with strong local gradients near half radius.

2. The experiment

A database of 37 near-identical discharges ($n_{\rm e}^{\rm av} = 3 \times 10^{19}\ {\rm m}^{-3}$, $B_\phi = 2.26$ T, $I_{\rm p} = 80$ kA, $q_{\rm a} = 5.1$) with far off-axis ($\rho_{\rm dep} \approx .55$) ECH ($P_{\rm ECH} \approx 350\,{\rm kW}$ in $2^{\rm nd}$ harmonic X-mode, injected in the horizontal midplane, from the low field side) is used for this study. The ECH pulse length is $150\,{\rm ms}$. The absorbed ECH power exceeds the Ohmic input power by a factor 5 in the ECH phase. A double pulse Thomson scattering diagnostic measures $T_{\rm e}$ and $n_{\rm e}$ profiles. The 2 measurements (separated 20 to $800\,\mu{\rm s}$ in time) are carried out simultaneously at 350 spatial points along a vertical chord of $300\,{\rm mm}$ with a resolution of $3\,{\rm mm}$ FWHM. $T_{\rm e}(t)$ is measured with an ECE radiometer. The $T_{\rm e}$-fluctuations are measured with the ECE imaging system.

In Fig. 1, the central temperature $T_{\rm e}(\rho = 0)$ is plotted vs. time for two typical discharges. ECH-power is switched on at $\delta t = -150\,{\rm ms}$. After $50\,{\rm ms}$ a steady-state hollow $T_{\rm e}$-profile and a corresponding hollow j-profile have formed [2, 3]. This paper focuses on the relaxation-process after switch-off of the ECH-power, in which two distinct states develop. These states equilibrate and remain separated until the end of the discharge ($viz. > 30$ electron energy confinement times and 4 to 5 current diffusion times). The high $T_{\rm e}$ discharges will be refered to as state I and the low $T_{\rm e}$-discharges will be refered to as state II. State I discharges form directly after the occurence of an off-axis sawtooth phenomenon, that often displays a $q = 2$ precursor [4].

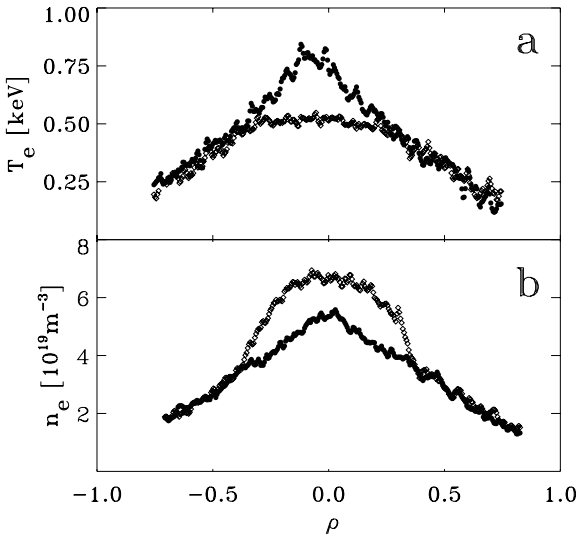

Figure 3. Thomson scattering $T_{\rm e}$-profiles (a) and $n_{\rm e}$-profiles measured at $\delta t = 75$ ms for both states (state I closed symbols, state II open symbols).

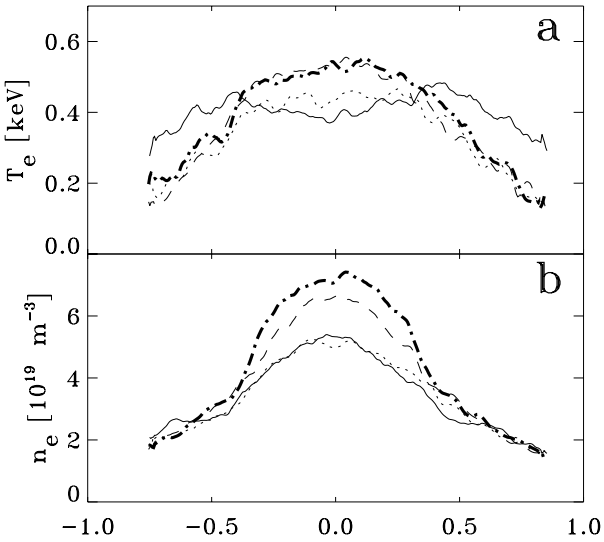

Figure 4. State II profiles at $\delta t = 0$ ms (full), 3 ms (dotted), 20 ms (dashed) and 35 ms (fat dashed-dotted) $T_{\rm e}(\rho)$ (a) adapts within the first 10 ms, whereas the changes in $n_{\rm e}(\rho)$ (b) take more than 35 ms.

In Fig. 2 the frequency of $T_{\rm e}(0)$ in the equilibrated post ECH phase of the discharges is plotted as a histogram with intervals of 22 eV each. The existence of the two states is clearly borne out by the data: a gap of 3 intervals with zero-occurence forms around 600 eV. Detailed analysis of the state I discharges indicates that the high $T_{\rm e}$-ensemble is in fact a compilation of two substates, packed so closely together that their differences cannot be appreciated from Fig. 2.

The equilibrated (see the dashed line in Fig. 1) $T_{\rm e}$- and $n_{\rm e}$-profiles as measured with Thomson scattering for state I and state II discharges are presented in Fig. 3. State I- (closed symbols)

and state II- (open symbols) profiles are similar in the outer regions ($\rho > .4$), and diverge in the centre. The state I discharges are identical to the pre-ECH discharges, which in RTP are characterised by triangular $n_{\rm e}$ and $T_{\rm e}$-profiles. The state II $T_{\rm e}$-profiles are flat in the core. The state II $n_{\rm e}$-profiles exhibit a steep gradient which develops at $\rho \approx .4$ outside of which the profiles are similar. The onset of the steep $\nabla n_{\rm e}$-region in state II is different from the onset of the high $\nabla T_{\rm e}$ region in state I (*viz.* .38 vs. .32). State II has less peaked pressure profiles than state I. The Ohmic power deposition is 130 kW for state I and 165 kW state II discharges. The electron energy confinement time $\tau_{\rm Ee}$ is 4.4 ms for state I and 4.2 ms for state II.

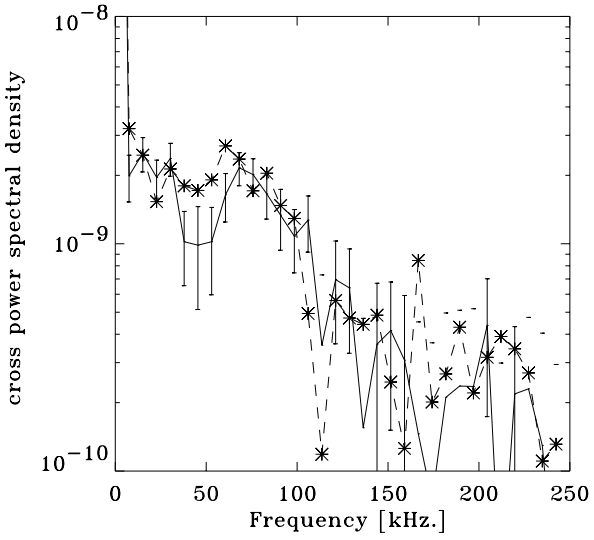

Figure 5. Cross power spectral density of $\tilde{T}$. The error bars denote the standard deviation over multiple realisations. It is seen that, within error bars, the spectra are tha same for the two states.

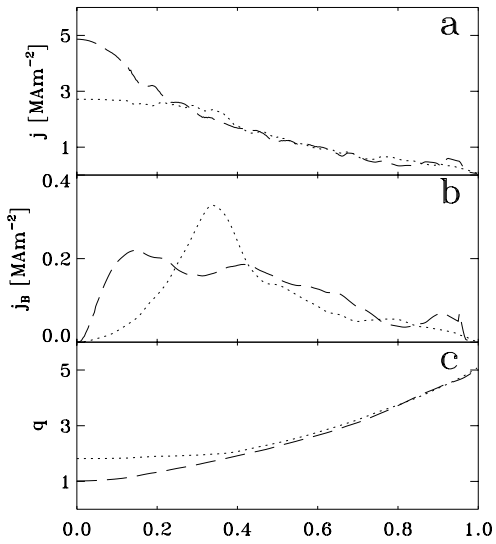

Figure 6. Profiles of the total current density $j(\rho)$ (a), bootstrap-current profile $j_{\rm B}(\rho)$ (b) and the safety factor $q(\rho)$ (c) for both states (state I dashed, state II dotted).

In Fig. 4 $T_{\rm e}$ (a) and $n_{\rm e}$-profiles (b) obtained at $\delta t = 0, 3, 20$ and $35\,{\rm ms}$ (full line, open symbols, closed symbols and squares respectively) are presented for discharges with similar prelude phases. After switch-off, the off-axis maximum in $T_{\rm e}$ is not supported and $T_{\rm e}(\rho > \rho_{\rm dep})$ decreases within the first 3 ms. $T_{\rm e}(0)$ slightly increases. Note the localized increase of $\nabla n_{\rm e}$ around $\rho = .38$ after switch-off. In the transition from state I to state II the quantity $\eta_{\rm e}(0)$ varies from 2.1 (critical) to .3 (sub-crittical). $\eta_{\rm e}$ is associated with a specific form of electrostatic turbulence, proposed as a candidate to explain the anomalous electron thermal transport. The variation in $\eta_{\rm e}$ is not reflected in the $\tilde{T}_{\rm e}$-spectra (see Fig. 5) as measured with the new ECE-imaging system. The spatial resultion of the system is 1.3 cm. The traces are subdived in in several realisations, for which the spectra can be determined. The standard deviation of the ensemble of realisations is an estimator for the error in the fluctuation spectra (see also B.H. Deng, this conference).

In equilibrium, the current-density $j(\rho)$ (see Fig 6a) can be calculated from $T_{\rm e}$ and $p_{\rm e}$ assuming neo-classical resistivity. In leading order, the bootstrap current (see Fig. 6b, state I dashed, state II dotted) is driven by $\nabla n_{\rm e}$ and the effect of the steep $\nabla n_{\rm e}$-region for state II discharges is clearly visible. The effect of the bootstrap current is that, in addition to the effect of the flat $T_{\rm e}$ region, the q-profile (see Fig. 6c) remains flat out to $\rho = .38$ for state II discharges with $q_{\rm min} \approx 1.8$. For state I discharges $q_{\rm min} \approx 1$.

3. Discussion

Both during off-axis ECH and in the relaxed Ohmic states, profile consistency [5-7] is not observed in our experiments. A wide variaty of profile shapes can be produced. The relationship $j\nabla p/p\nabla j$ (associated with PC) changes in the transition from state II to state I. For discharges with equal $n_{\rm e}$, the central confinement properties of the state I discharges are superior to the central confinement of state II discharges. The variation of $\eta_{\rm e}$ is therefore not reflected in the confinement properties of the two states. The variation of $\eta_{\rm e}$ is also not reflected in the high frequency part of the $\tilde{T_{\rm e}}$-spectra.

Recent experiments carried out in RTP indicate that in EC-heated discharges, barriers for the electron thermal transport are present near $q = 7/2, 3/1, 5/2, 2/1, 3/2, 4/3$ and $1/1$ [1]. With such barriers, the discharge evolution is critically dependent on small local variations of j which lead to variations in $\hat{s}$ and to significant variations in $\chi_{\rm e}$. The observation of bifurcted Ohmic states would be consistent with this picture if we assume that the barriers are not formed, but merely high-lighted by the ECH. A code with q-related barriers, that reproduced the plasma behaviour during ECH up to great detail, also reproduced the state II $T_{\rm e}$ profiles when the density profile was forced to peak [8]. When the density profile was not forced to peak, the state I profiles were reproduced. Self-organisation of the $T_{\rm e}$-profiles occurs through the following mechanism: A wide $T_{\rm e}$-profile leads to a wide j-profile and a relatively high q_0. The central barrier doesn't form and the $T_{\rm e}$-profile remains flat. A peaked $T_{\rm e}$-profile a relatively low q_0. The central barrier does form and the $T_{\rm e}$-profile remains flat.

The behaviour of the $n_{\rm e}$ profiles is not understood. In steady-state a local balancing between inward convective particle fluxes, ionisation of influxing neutrals and outward diffusion exists. Influx of neutral particles can be ruled out as an explanation for the differences in the two states, because 1) the neutrals stem from the edge region of the plasma where both states feature similar conditions and 2) neutral influx can never explain such a localized increase of $\nabla n_{\rm e}$. The formation should therefore be due to a reduction of the local particle diffusion coefficient, an increase of the inward particle convection or a conbination of the two effects. Sofar we are not able to distinguish between these effects.

Acknowledgements

Prof. Dr. F.C. Schüller and Dr. A.A.M. Oomens are acknowledged for stimulating discussion, the RTP-team for machine and diagnostic operation. This work was done under the Euratom-FOM association agreement with financial support from NWO and Euratom.

References

[1] N.J. Lopes Cardozo et al.: Plasma Phys. Control. Fusion **39** (1997) B303-B316
[2] G.M.D. Hogeweij et al.: Phys. Rev. Lett. **76** (1996) 632
[3] M.R. de Baar et al.: Phys. Rev. Lett. **78** (1997) 4573
[4] M.R. de Baar et al.: "Bifurcated states of ohmially heated tokamak", *submitted to* Phys. Rev. Lett.
[5] B. Coppi: Comm. Plasma Phys. Contr. Fusion **5** (1980) 261
[6] J.B. Taylor: Phys. Fluids B **5** (1993) 4378
[7] B.B. Kadomtsev: Izv. VUZov **29** 1032
[8] G.M.D. Hogeweij, N.J. Lopes Cardozo, and M.R. de Baar: "A model for electron transport barriers in tokamaks, tested against experimental data in RTP", *submitted to* Nucl. Fus.